Analysis of Electromagnetic Forces in Skewed Electric Drives in the Full Operating Range

Matthias Boesing, Thomas Schniedertoens, and Rik W. De Doncker
Institute for Power Electronics and Electrical Drives of RWTH Aachen University
Jaegerstr. 17/19, 52066 Aachen, Germany bs@isea.rwth-aachen.de

***Abstract*—Torque and radial force fluctuations in highly utilized permanent magnet machines are strongly operating point dependent. In speed-variable drives, they need to be calculated for the entire operating range. This paper shows how skew can be accounted for with negligible additional effort. The simulation points are suitably distributed in the dq-current plane and subsequently superposed. Applying this technique to an electric vehicle drive, it is shown that operating points occur where the skew effect deviates strongly from its analytical approximation. The one-slot skew angle eventually becomes counterproductive for force ripple reduction and acoustic noise increases.**

I. Introduction

When analyzing skewed machines using multi-slice methods in 2-D FEM [1]–[3], single operating points are typically investigated. In highly utilized interior permanent magnet machines (PMSM), torque and radial force fluctuations are strongly operating point dependent. The resulting acoustic noise is critical in electric vehicles. Simulations need to be performed for all operating points. Without further consideration the computational effort increases proportionally to the number of slices. It is shown in this paper how by suitable distribution of the operating points in the dq-current plane, (discontinuous) skew can be accounted for with negligible additional effort. Furthermore it is shown that in certain operating points, the skew effect deviates from its analytical approximation and the ripple components increase.

The analysis here considers a $p = 5$ pole PMSM with $q = 2$ slots per pole per phase. For the given machine, one slot skew ($30°\mathrm{el}$) is a typical choice for reducing the strongest shape 0 (spatially constant) ripple component (i.e. torque ripple and radial force excitation in a 'breathing' shape [4]) at the 60. multiple of the mechanical frequency f_{mech} [5].

II. Analytical Description of Discontinuous Skew

We start with the idealizing assumption that the force on the slices is identical. Then a functional expression between the shape 0 forces $f_{\mathrm{n,skewed}}(t)$ in skewed machines and $f_{\mathrm{n,unskewed}}(t)$ in unskewed machines can be expressed by the skew function $h_{\mathrm{skew}}(t)$ as

$$f_{\mathrm{n,skewed}}(t) = h_{\mathrm{skew}}(t) * f_{\mathrm{n,unskewed}}(t,\theta) \tag{1a}$$

$$\Updownarrow$$

$$F_{\mathrm{n,skewed}}(f,\theta) = H_{\mathrm{skew}}(f) \cdot F_{\mathrm{n,unskewed}}(f,\theta). \tag{1b}$$

Basically extending an approach shown in [6] towards discontinuous skew with n slices (n odd here), $h_{\mathrm{skew}}(t)$ and $H_{\mathrm{skew}}(f)$ can be written as

$$h_{\mathrm{skew}}(t) = \frac{1}{n}\sum_{k=1}^{n}\delta\left(t - \frac{(n+1)T}{2n} + k\frac{T}{n}\right) \tag{2a}$$

$$\Updownarrow\ (n \text{ odd})$$

$$H_{\mathrm{skew}}(f) = \frac{1}{n} + \frac{2}{n}\sum_{k=1}^{\frac{n-1}{2}}\cos\left(2\pi f T\frac{k}{n}\right) \tag{2b}$$

where $T = 1/60 f_{\mathrm{mech}}$, here. $H_{\mathrm{skew}}(f)$ is zero at $60 f_{\mathrm{mech}}$ so that under the idealizing assumption made above, this main noise component would cancel out completely and in reality a significant reduction is expected.

III. Skew Simulation Procedure

A. General Setup

Distributing the simulated operating points in the dq-current space in a polar coordinate system (i.e. varying control angle γ and current amplitude i_{s}) allows to account for skewed machines without relevant additional effort. The simulated operating points in the dq-current plane are shown in Fig. 1. Each star represents one simulation. For every simulation the rotor is stepped until the results can be expanded due to symmetry. The angular distance γ between the different operating points was set to $10°\mathrm{el}$. The peak phase current i_{s} varies between $1/6\, i_{\max}$ and $i_{\max}$. With this simulation setup, the entire operating area can be simulated and analyzed.

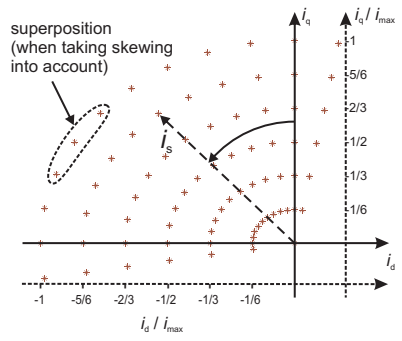

Fig. 1. Operating point distribution in the dq-current plane

B. Result Superposition to Account for Skew

Discontinuous one-slot skew with 3 segments leads to a displacement of $10°\mathrm{el}$ between the slices. Therefore, in order to obtain the results for one operating point of the skewed machine, three simulations are superposed as shown in Fig. 1. The results can be calculated from

$$\xi_{\mathrm{results}} = \frac{\xi_{\gamma-10°\mathrm{el}} + \xi_{\gamma} + \xi_{\gamma+10°\mathrm{el}}}{3} \tag{3}$$

with the control-angle γ and the result quantity ξ. Only the operating points at $\gamma = -10°\mathrm{el}$ and $\gamma = 100°\mathrm{el}$ are simulated additionally to generate results for the skewed version of the machine. Applying a control strategy to the machine, the results are mapped from the dq-current to the torque-speed plane [4].

IV. Results

A. Force and Torque in Time Domain

Fig. 2 shows radial force and torque in the time domain for one operating point ($i_{\mathrm{s}} = i_{\mathrm{max}}$, $\gamma = 50°\mathrm{el}$). The x-axis is spaced in electrical degrees so that its spacing is speed independent. The forces in the radial direction for the 3 slices of the unskewed version are colored in black. It is apparent that in contrast to the simplifying assumption in section II they are not only phase shifted, in particular due to the DC offset. However, neglecting their DC offset they are indeed fairly similar with the expected phase shift. The superposition of the operating points (colored in red) represents the skewed version of the machine. For this operation point, skew reduces the shape 0 force ripple and as a consequence reduces the noise emission of the machine compared to the unskewed version of the machine (black solid line).

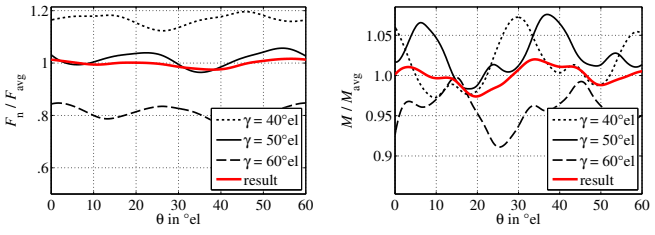

(a) radial force in time domain (b) torque

Fig. 2. Effects of rotor skew on forces and torque in time domain

B. Effect of Skew for the Entire Operating Range

The effect of skew on the main radial force component at $60 f_{\mathrm{mech}}$ [5] is evaluated for the entire operating range. Fig. 3 shows the difference in the force excitation between skewed and unskewed machine. The difference is calculated as

$$\Delta A_{\mathrm{r},0,60} = A_{\mathrm{r},0,60}|_{\mathrm{skewed}} - A_{\mathrm{r},0,60}|_{\mathrm{unskewed}}. \tag{4}$$

where $A_{\mathrm{r},0,60}$ is the radial shape 0 force excitation at $60 f_{\mathrm{mech}}$ (after spatial and temporal decomposition of the force excitation as shown in [4]). A negative result represents a reduction of the noise emission which is equivalent to a greenish color in Fig. 3.

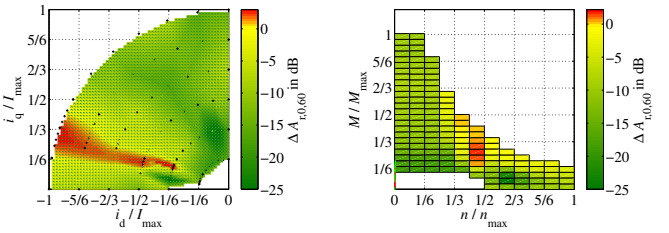

(a) in dq-current plane (b) over torque and speed

Fig. 3. Radial force reduction (shape 0, 60^{th} harmonic order)

Fig. 3(a) shows for the dq-current plane that rotor skew reduces the radial force ripple in almost all operating points. Improvements of more than $-20\ \mathrm{dB}$ can be achieved. However, around $\gamma = 70°\mathrm{el}$ (red region in Fig. 3(a)) the force magnitude slightly increases when skewing the rotor. To better capture this effect, additional operating points (higher density of '+' symbols) have been calculated in that region.

The same results mapped to the torque-speed plane are shown in Fig. 3b. In the base-speed range (typical operating range for servo drives), significant improvements are visible. However, the acoustically most critical operating points for traction drives are typically along the constant power line in the field-weakening regime. There, the effect of skew is significantly lower. Around $n_{\mathrm{max}}/2$, rotor skew even increases the air-gap forces. The simplifying analytical approximation from section II does no longer hold and saturation effects are apparent.

V. Conclusion

Suitable distribution of the simulated operating points allows to account for skew without relevant additional effort. It is shown that for assessing the effectiveness of a certain skew angle in highly utilized drives, the entire operating range needs to be investigated. Significant deviation from the ideal effect occurs and force and torque ripple may even increase.

References

[1] J. Gyselinck, L. Vandevelde, and J. Melkebeek, "Multi-slice FE modeling of electrical machines with skewed slots-the skew discretization error," *Magnetics, IEEE Transactions on*, vol. 37, no. 5, pp. 3233 –3237, Sep. 2001.

[2] M. Henschel, "Berechnung und Optimierung permanenterregter Maschinen am Beispiel von Generatoren für Windkraftanlagen," Ph.D. dissertation, Technische Universität Darmstadt, 2006.

[3] C. Schlensok, A. Kelleter, and K. Hameyer, "Skew-discretization error for structural dynamic finite element simulations of electrical machines," in *COMPUMAG 2005*, Shenyang, China, June 2005.

[4] M. Boesing, T. Schoenen, K. Kasper, and R. De Doncker, "Vibration synthesis for electrical machines based on force response superposition," *Magnetics, IEEE Transactions on*, vol. 46, no. 8, pp. 2986 –2989, 2010.

[5] M. Boesing, K. Kasper, and R. De Doncker, "Vibration excitation in an electric traction motor for a hybrid electric vehicle," in *Proceedings of the 37th International Congress and Exposition on Noise Control Engineering, INTER-NOISE 2008*, Shanghai, China, Nov. 2008.

[6] D. Hanselman, "Effect of skew, pole count and slot count on brushless motor radial force, cogging torque and back emf," *Electric Power Applications, IEE Proceedings* -, vol. 144, no. 5, pp. 325 –330, Sep. 1997.